ARTICLE
Journal of Cellular Biochemistry 113:184–193 (2012)

Journal of Cellular Biochemistry

Identification and Characterization of a Bactericidal and Proapoptotic Peptide From *Cycas revoluta* Seeds With DNA Binding Properties

Santi M. Mandal,[1] Ludovico Migliolo,[2] Subhasis Das,[3] Mahitosh Mandal,[3] Octavio L. Franco,[2*] and Tapas K. Hazra[1]

[1] *Department of Internal Medicine, University of Texas Medical Branch, Galveston, Texas 77555*

[2] *Centro de Análises Proteômicas e Bioquímicas, Pós-Graduação em Ciências Genômicas e Biotecnologia UCB, Brasília-DF, Brazil*

[3] *School of Medical Science and Technology, Indian Institute of Technology, Kharagpur 721 302, West-Bengal, India*

ABSTRACT

Nowadays, novel pharmacies have been screened from plants. Among them are the peptides, which show multiple biotechnological activities. In this report, a small peptide (Ala–Trp–Lys–Leu–Phe–Asp–Asp–Gly–Val) with a molecular mass of 1,050 Da was purified from *Cycas revoluta* seeds by using reversed-phase liquid chromatography. This peptide shows clear deleterious effects against human epidermoid cancer (Hep2) and colon carcinoma cells (HCT15). It caused inhibition of cancer cell proliferation and further disruption of nucleosome structures, inducing apoptosis by direct DNA binding. A remarkable antibacterial activity was also observed in this same peptide. Nevertheless, no significant lysis of normal RBC cells was observed in the presence of peptide. Additionally, an acetylation at the N-termini portion is able to reduce both activities. Bioinformatics tools were also utilized for construction of a three-dimensional model showing a single amphipathic helix. Since in vitro binding studies show that the target of this peptide seems to be DNA, theoretical docking studies were also performed to better understand the interaction between peptide and nucleic acids and also to shed some light on the acetyl group role. Firstly, binding studies showed that affinity contacts basically occur due to electrostatic attraction. The complex peptide-ssDNA was clearly oriented by residues Ala[1], Lys[3], and Asp[6], which form several hydrogen bonds that are able to stabilize the complex. When acetyl was added, hydrogen bonds are broken, reducing the peptide affinity. In summary, it seems that information here provided could be used to design a novel derivative of this peptide which a clear therapeutic potential. J. Cell. Biochem. 113: 184–193, 2012.

KEY WORDS: PLANT PEPTIDES; ANTICANCER PEPTIDE; MOLECULAR MODELING; DNA AFFINITY; ANTIMICROBIAL PEPTIDES

Numerous polypeptides possess a biological activity that makes them potential drugs. Among them are included the anticancer agents. For this reason, several peptides have been evaluated and are now in clinic trials of phase II and III in order to treat tumor cells [Torchilin and Lukyanov, 2003]. Moreover, several advanced techniques have been developed to kill cancer cells, despite the efficiency of chemotherapy and, more recently, biochemotherapy, especially for metastatic disease stages [Espinosa et al., 2004]. While some agents are completely unspecific, causing several collateral effects, some peptides have been screened since they can directly act on target cells and/or will elicit an immune response that may be effective to control infections and reduce tumor development. Furthermore, peptides have also attracted attention as drug candidates owing to their possession of certain key advantages over alternative chemotherapy molecules. Peptides allow structural changes to incorporate protective

Abbreviations: *Cr*-ACP1, *Cycas revoluta*-anticancerous peptide 1; *Cr*-AcACP1, *Cycas revolute* acetylated anticancerous peptide 1; FBS, fetal bovine serum; Hep2, human epidermoid cancer cells; MALDI-ToF MS, matrix assisted laser desorption ionization time of flight mass spectrometry; MEM, minimum essential medium; MTT, 3-(4,5-dimethylthiazol-2-yl)-2,5-diphenyltetrazolium bromide; MMP, mitochondrial membrane potential; PI, propidium iodide; Rho123, Rhodamine123; RP-HPLC, reversed-phase high performance liquid chromatography; ssDNA, single stranded DNA.

Santi M. Mandal's present address is Central Research Facility, Indian Institute of Technology, Kharagpur 721 302, West-Bengal, India.

*Correspondence to: Octavio L. Franco, SGAN 916N, Modulo C, sala 219, Brasilia, Distro Federal 70990-100, Brazil. E-mail: ocfranco@gmail.com, ocfranco@pos.ucb.br

Received 29 May 2011; Accepted 23 August 2011 • DOI 10.1002/jcb.23343 • © 2011 Wiley Periodicals, Inc.
Published online 31 August 2011 in Wiley Online Library (wileyonlinelibrary.com).

substitutions, chiral derivatives, non-natural amino acids, and other modifications aiming at increased stability, efficiency, and resistance to proteolysis [Otero-Gonzalez et al., 2010; Gong et al., 2011]. Several hundred peptide sequences with biological activity have been recognized and a few of them are in clinical trial [Rawat et al., 2006]. Finally, peptide-based vaccines are now in development for various pathologies including cancer [Roy et al., 2010].

Among the various goals of anticancer pharmacies, DNA is a main target for numerous antitumor drugs [Purcell et al., 2007]. Reversible or irreversible modifications of the nucleic acids can lead to disruption of the transcription and/or replication, initiating ultimately the death of cancer cells [Mader et al., 2011]. The development of functionalities that bind DNA is of prime importance in cancer chemotherapy and design of synthetic peptide. The inherent dark toxicity and cellular resistivity have generated subsequent interest to develop a new generation of DNA binding peptide-based anticancer agents. On other hand, the structural changes of DNA based on the interaction of small molecular mass ligands with deoxyribonucleic acid have attracted attention in the medicinal design of anticancer and anti-AIDS drugs [Rees et al., 1993; Sartorius and Schneider, 1995; Yang and Wang, 1996]. Additionally to common peptide screening, in vitro and in silico studies of small oligopeptides may shed some light on these processes, by providing simple systems where molecular interactions can be characterized in detail. However, to date, little emphasis has been placed on tailoring the coordinated peptides to a DNA-binding activity in vitro and in silico. The present study was undertaken to identify a naturally occurring seed peptide capable of inhibiting the growth of cancer cells, and to investigate its biologic behavior to bind DNA in vitro and in silico. Different peptide database (http://aps.unmc.edu/AP/main.php) possess various peptides with anticancer activity [Rozek et al., 2000; Perera et al., 2009; Wu et al., 2009; Feliu et al., 2010]. Nevertheless, only a few of them have been isolated from plant seeds and also show activity against human epidermoid cancer (Hep2) cells [Paganuzzi et al., 1985], as most of them were not clearly evaluated according to their mechanism of action. Furthermore, very little structural characterization by homology modeling and docking studies was observed in the literature [Tan et al., 2009].

Another interesting issue observed in the literature is peptide promiscuity, in which multiple functions are associated with a single molecule [Franco, 2011]. This property is also extremely desirable for drug development. Among multiple functions, several plant peptides have shown antimicrobial activity [Mandal et al., 2009; Otero-Gonzalez et al., 2010; Moreira et al., 2011; Ribeiro et al., 2011] but few peptide groups are able to control tumors and pathogens at the same time [Ireland et al., 2010]. This is much more commonly observed in peptides from animal sources such as crotamine [Kerkis et al., 2010] and LL-37 [Mader et al., 2011]. In addition to these facts, the *Cycas revoluta* have been studied in last few years as an important source of proteinaceous compounds with biotechnological potential as antifungical, antibacterial, and antitumors [Yokoyama et al., 2008, 2009]. With this in mind, this report describes the isolation of a novel peptide from *C. revoluta* seeds, here synthesized in acetylated and non-acetylated forms, with antitumor activities against Hep2 and human colon carcinoma (HCT15) cells. Nevertheless, no significant lysis of normal RBC cells was observed in the presence of peptides. Aiming to evaluate the acetylation effects over *C. revoluta* peptide DNA binding properties a modified peptide was produced containing two acetyl groups since several reports showed that acetyl groups could be effective for regulation of chromatin structure and function, and sometimes the acetylated form showed a dramatic effect on DNA binding properties [Johnson and Turner, 1999]. Peptide-DNA complexes were observed and an in silico explanation by molecular modeling and docking was provided. Finally, a secondary antimicrobial activity was obtained, showing a possible multifunctionality in a single peptide.

MATERIALS AND METHODS

SAMPLE PREPARATION

Mature seeds of *C. revoluta* were collected from different plants grown on the University of Texas Medical Branch campus, USA. The seeds were individually cracked and ground to flour. Thirty grams of the seeds were extracted with 100 ml of phosphate-buffered saline (0.1 M PBS, pH 7.4) containing protease inhibitor cocktail (Sigma). The extraction mixture was shaken for 48 h at 4°C, and centrifugation of the protein extract took place at 12,000*g* for 30 min. Peptides less than 3 kDa were extracted from the supernatants using a 3 kDa cut-off membrane (Millipore) and further lyophilized. Dry samples were dissolved in 1 ml of 5% (v/v) acetonitrile solution containing 0.01% (v/v) trifluoroacetic acid (TFA).

PEPTIDE PURIFICATION

Samples were fractionated by using reversed-phase HPLC (Agilent 1100 series) with a ZORBAX-300SB-C18 column (4.6 mm × 150 mm, particle size 5 mm), at a flow rate of 600 μl min^{-1}, by using a linear acetonitrile gradient (5–60%, v/v) for 120 min at 30°C. TFA at 0.04% (v/v) was used as ion pairing agent. The elution was monitored at 220 nm with a UV/DAD detector (DAD, G1315B). Selected fractions of the HPLC chromatogram were collected using a coupled fraction collector (GILSON, France). Individual fractions were concentrated by Speed-Vac. The target fraction, which showed anticancer activity, was re-chromatographed in the same column, at a flow rate of 600 μl min^{-1}, under isocratic elution with 55% (v/v) acetonitrile containing 0.04% (v/v) TFA. The elution was monitored at 220 nm. Selected fractions were collected and processed for further studies.

MASS SPECTROMETRY ANALYSIS

Purified lyophilized peptide was resuspended in reduction and alkylation buffer (0.5 M Tris-buffer pH 8.0, 6 M guanidine hydrochloride, 1 mM DTT, and 20 mM EDTA) to a concentration of 1 mg ml^{-1}. The solution was overlaid with N2 gas and then incubated at 55°C for 2.5 h. Again, freshly prepared 0.5 mM DTT was added and incubated for another hour. The solution was cooled to room temperature for 10 min, and iodoacetamide was added to buffer for a final concentration of 3 mM and incubated for 10 min in the dark. The lyophilized peptides were resuspended in 5% (v/v) acetonitrile solution containing 0.01% (v/v) TFA. Two microliters of peptide solution was mixed with 24 μl of α-cyano-4-hydroxycin-

namic acid (CHCA) 10 mg ml^{-1}, used as matrix. Then, 1.0 μl sample was spotted onto the MALDI 100-well stainless steel sample plate and allowed to air dry prior to the MALDI analysis [Mandal et al., 2009, 2010]. A Voyager Time-of-Flight mass spectrometer (Applied Biosystems, Foster City, CA) was used to obtain MALDI mass spectra equipped with 337 nm N2 laser and operated in accelerating voltage 20 kV. The spectra were recorded in the positive ion linear mode. Reproducibility of the spectrum was checked five times from separately spotted samples.

AMINO ACID SEQUENCING

HPLC fractions were lyophilized and resuspended in 5% acetic acid, and the fraction was submitted for amino acid sequencing by Edman degradation at the UTMB Peptide Sequencing Facility. "After sequencing, the peptide was designated as Cr-ACP1."

PEPTIDE SYNTHESIS

Peptide synthesis reagents including Fmoc amino acids (AnaSpec Inc., San Jose, CA) and coupling solvents (PE Biosystems, Applied Biosystems) were used to synthesize the peptide on an ABI 431A peptide synthesizer (Applied Biosystems) using double coupling for all residues. The scale of synthesis was 0.25 mmol and synthesized by the UTMB peptide synthesis core facility. After cleavage, the resuspended peptide was further purified by reversed-phase high performance liquid chromatography (RP-HPLC) using the same gradient program as described above in purification of the native peptide. The major peak was lyophilized and its purity checked by matrix assisted laser desorption ionization time of flight mass spectrometry (MALDI-ToF-MS) analysis with matrix α-cyano in proportion 3:1 matrix-sample.

PEPTIDE ACETYLATION

Two milligrams of peptide was reconstituted with 200 μl of 50 mM ammonium bicarbonate buffer and 500 ml of acetylation reagent (200 μl acetic anhydride + 600 μl methanol). The reaction was left at room temperature for 1 h. Methanol and unreacted acetic anhydride were then removed with Speed-Vac and lyophilized. The resulting acetylated peptide was confirmed by MALDI-ToF-MS and was futher denominated Cr-AcACP1.

BACTERICIDAL ASSAYS

S. epidermidis, *Bacillus subtilis*, *Pseudomonas aeruginosa*, and *Escherichia coli* ATCC 8739 were used for antimicrobial bioassays. The bacterial species were cultured in 1.0 ml LB broth (10 g L^{-1} NaCl, 5 g L^{-1} yeast extract, and 45 g L^{-1} bactopeptone) for 2 h, at 37°C. Acetylated and non-acetylated peptides were re-suspended in 50 mM PBS (pH 7.4), filtered through 0.22 μm nylon membranes, and incubated at 512 and 100 μg ml^{-1} final concentrations, respectively, with 5×10^6 CFU ml^{-1} of each bacterial species for 4 h, at 37°C. PBS (pH 7.4) and chloramphenicol (40 μg ml^{-1}) were used as negative and positive controls, respectively. Bacterial growth was measured at 595 nm, every hour within the period of incubation, carried out according to protocols described by the National Committee for Clinical Laboratory Standards guidelines [Wikler et al., 2005]. Each experiment was carried out in triplicate. In addition, to determine the MIC value, purified peptides were serially diluted from 256 to 2 μg ml^{-1} in LB medium. In each well of a 96-well polypropylene plate, 100 μl of each peptide dilution and 10 μl of cell suspension of bacteria were added (approximately 5×10^6 CFU of bacteria). The plates were incubated for 12 h at 37 °C. During this period the absorbance was measured in a plate reader (Bio-Rad 680 Microplate Reader) at 595 nm every 30 min.

CYTOTOXICITY ANALYSIS

Hep2, non-carcinoma mouse embryo fibroblast cells (NIH 3T3) and HCT15 cells were obtained from the National Center for Cell Sciences (Pune, India). The cells were cultured as monolayers in minimum essential medium (MEM) supplemented with 10% (v/v) heat-inactivated fetal bovine serum (FBS) and antibiotics, and incubated at 37°C in a humidified atmosphere of 95% air and 5% CO_2. Cells were plated at a density of 2,500 cells per well in a 96-well flat-bottomed plate and allowed to attach to the culture surface overnight. At the next day, broth was aspirated off, washed with PBS (1×) buffer and 200 μl of each peptide-containing (0–4.0 mM) medium were separately added in triplicates. After 72 h incubation, the medium was newly aspirated off and washed with PBS (1×) buffer, following the addition of 50 μl of 3-[4,5-dimethylthiazol-2-yl]-2,5-diphenyltetrazolium bromide (MTT reagent) at a standard concentration of, 3 mg ml^{-1} to each well and further incubating for 3 h. At the end of the incubation, the MTT-containing medium was aspirated off and once more washed with PBS (1×) buffer and then 200 μl of DMSO solution was added to each well. After 10 min, optical density was determined using a MultiSkan plate reader (LabSystems) at a wavelength of 570 nm.

CELL CYCLE ANALYSIS

Cells were seeded at an equal density per dish and allowed to adhere. After 24 h, cells were synchronized at G1 phase in complete medium supplemented with 2% FBS (for 24 h) according Kues et al. [2000] and further treated with the different peptide concentrations along with the control (0.1% DMSO). After treatment, cells were collected and washed in PBS and incubated in 70% ethanol for 45 min at 4°C or kept at −20°C overnight for fixation. Cells were centrifuged, washed, and then incubated with PI solution (40 μg ml^{-1} PI, 100 μg ml^{-1} RNase A in PBS) at 37°C for 1 h. Apoptotic cells were determined by their hypochromic sub-diploid staining profiles. The distribution of cells in the different cell cycle phases was analyzed from the DNA histogram using Becton–Dickinson FACSCalibur flow cytometer and Cell Quest Pro software.

MICROSCOPIC ANALYSIS

Hep2 cells were treated with different concentrations of *Cr*-ACP1 and *Cr*-AcACP1 (0–4 mM) for 48 h. Cells were washed with PBS. Afterwards, 1 μl of aqueous solution of ethidium bromide (EB, 100 μg ml^{-1}) was added and the cell types were observed under a fluorescence microscope (Olympus, Tokyo, Japan).

ELECTRO MOBILITY SHIFT ASSAY

Electrophoretic mobility shift assay (EMSA) was performed to examine the peptide's DNA binding activity. Synthetic peptides, *Cr*-ACP1, and *Cr*-AcACP1 of 0, 0.8, and 1.0 mM concentration with a 5′-P32-labeled containing 2 nM oligo (5′-CCG GCG CAG GGC TTA

GGT CT-3′) were incubated in 10 μl of reaction buffer containing 25 mM Hepes-KOH (pH 7.6), 50 mM NaCl, 0.5 mM EDTA, 0.5 mM DTT, and 12% glycerol at 20°C for 15 min, followed by electrophoresis at room temperature in a 6% non-denaturing polyacrylamide gel containing 25 mM Tris–HCl, pH 7.5, 55 mM borate, and 0.6 mM EDTA. The radioactivity in the DNA protein complex was analyzed with a PhosphorImager (Molecular Dynamics).

HEMOLYTIC ASSAY

Hemocompatibility study was performed following the protocol by Mandal et al. [2011]. Briefly, RBC (from 6-week-old male BALB/c mice) suspension was added to HEPES-buffered saline (negative control), 1.0% Triton X-100 (positive control) and further incubated with 1 mM of *Cr*-ACP1 and *Cr*-AcACP1 peptides for 30 min at 37°C. After incubation, the supernatants were transferred to a 96-well plate. Hemolytic activity was determined by measuring the OD absorption at 570 nm. Control samples of 0% lysis (in HEPES buffer) and 100% lysis (in 1% Triton X-100) were considered in the experiment. All assays were performed in triplicate. Hemolytic effect of each treatment was expressed as percent cell lysis relative to the positive control using the following formula: $[(Abs_{570}$ of peptide)/$(Abs_{570}$ of positive control)$] \times 100$.

IN SILICO ANALYSES AND MOLECULAR MODELING

Initially, PSI-BLAST was used in order to find best templates for homology modeling no reliable data was obtained. I-Tasser server [Roy et al., 2010] was utilized for discovery templates. The pdb 1d9j [Oh et al., 1999] and 1b1v [Volkman et al., 1999] showed 45% and 23% of identity, respectively. Fifty theoretical three-dimensional (3D) peptide structures were constructed using multiple templates by Modeller v.9.8. The acetylated model was constructed in accordance with MALDI-ToF data. The acetyl groups were added to amino acid residues alanine (Ala^1) and lysine (Lys^3). The final models were evaluated: that is, geometry, stereochemistry, and energy distributions in the models were performed using PROSA II to analyze packing and solvent exposure characteristics and PROCHECK for additional analysis of stereochemical quality [Morris et al., 1992; Laskowski et al., 1996]. In addition, root main square deviation (RMSD) was calculated by overlap of Cα traces and backbones onto the template structure through the program 3DSS [Sumathi et al., 2006]. The protein structures were visualized and analyzed on SPDB viewer v.3.7 [Kaplan and Littlejohn, 2001] and Delano Scientific's PYMOL http://pymol.sourceforge.net/.

PEPTIDE–DNA DOCKING ANALYSIS

Molecular docking HEX v.5.1 [Ritchie, 2008] program was used to examine possible modes of interaction between the peptides that were acetylated and non-acetylated with single stranded DNA (ssDNA) 5′-CCGGC-3′. Briefly, this procedure performed global rotational and translational space scan by using Fourier transformations, which rank the output according to surface complementarity and electrostatic characteristics. A list of 50 complexes of peptide-ssDNA was ranked and evaluated according to spatial restraint, salt bridge formation, hydrogen bond, and hydrophobic interaction for both peptides. Validation was carried out according to biochemical data, stereochemical limitation, and formation length using the Pymol program for visualization. The interaction area was calculated through the number of contact points obtained from amino acid residues interaction.

RESULTS AND DISCUSSION

PEPTIDE ISOLATION AND CHARACTERIZATION

In order to isolate low molecular mass (<3 kDa) anticancer peptides from *C. revoluta*, crude extract was passed through a 3 kDa cut-off ultra filtration membrane and further applied onto a reversed phase chromatograph (RP-HPLC), Figure 1A shows the chromatographic profile of peptides purified from *C. revoluta*. The antiproliferative activity of each fraction was in vitro challenged against Hep2 cell lines. Seven peaks were detected and the peak eluted at 41 min showed higher antiproliferative activity against Hep2 cells in comparison to other HPLC fractions. MALDI-ToF-MS analysis of fraction 5 showed that the monoisotopic peptide molecular mass was 1050.89 (Fig. 1B). The peptide sequence obtained by Edman degradation procedure (data not shown) was Ala–Trp–Lys–Leu–Phe–Asp–Asp–Gly–Val (AWKLFDDGV) and was further named *Cr*-ACP1. Synthesized peptide after acetylated modification was named *Cr*-AcACP1, and was further confirmed by RP-HPLC and MALDI-ToF-MS analysis. The monoisotopic acetylated peptide molecular masses was 1092.94 and 1134.68, indicating that major quantity of *Cr*-AcACP1 peptide received two acetyl groups, being one of them linked to Ala^1 and the other to Lys^3 (Fig. 1C).

PROAPOPTOTIC ACTIVITY OF *Cr*-ACP1 AND *Cr*-AcACP1

Both the synthetic peptides, *Cr*-ACP1 and *Cr*-AcACP1, inhibited cell proliferation of Hep2, and colon carcinoma cell, HCT15 in a dose-dependent manner. Cell inhibition was prominent mainly at concentrations of 1–2 mM for *Cr*-ACP1 and 0.6–0.8 mM for *Cr*-AcACP1, as confirmed by MTT assay (Fig. 2a and c). The IC_{50} values of *Cr*-ACP1 and *Cr*-AcACP1 in Hep2 cells were 1.5 and 0.8 mM, respectively. So, the results were obtained from both Hep2 and HCT15 cells found to be in good agreement for the apoptotic activity of the peptides. Furthermore, the specificity of *Cr*-ACP1 and *Cr*-AcACP1 to cancerous cells was evaluated by comparing with a non-carcinoma mouse embryo fibroblast cell line NIH 3T3. Data here reported revealed that acetylated and non-acetylated peptides were less toxic to normal cells when compare to cancerous cell (Fig. 2e). Hemocompatibility study revealed the effectiveness of both the peptides where it showed no significant lysis of normal RBC cells compare to positive control (Fig. 2d).

Both peptides seem to induce cell cycle arrest at the G0–G1 phase of Hep2 cells, as shown in Figure 3. Several peptides have shown anticancer activities [Gong et al., 2011; Mader et al., 2011], but only a few of them have been purified from plants [Preza et al., 2010]. This study showed that peptides isolated from cacao seeds were capable of controlling murine lymphoma. Moreover, the groups of cyclic peptides known as cyclotides have also shown antitumor activities in addition to several other peptide functions [Ireland et al., 2010]. There were 23.69% and 59.05% relative increases for 24 h in the G0–G1 phase in epidermoid cancer cells with *Cr*-ACP1 and *Cr*-AcACP1 (0.8 mM), respectively, compared with control

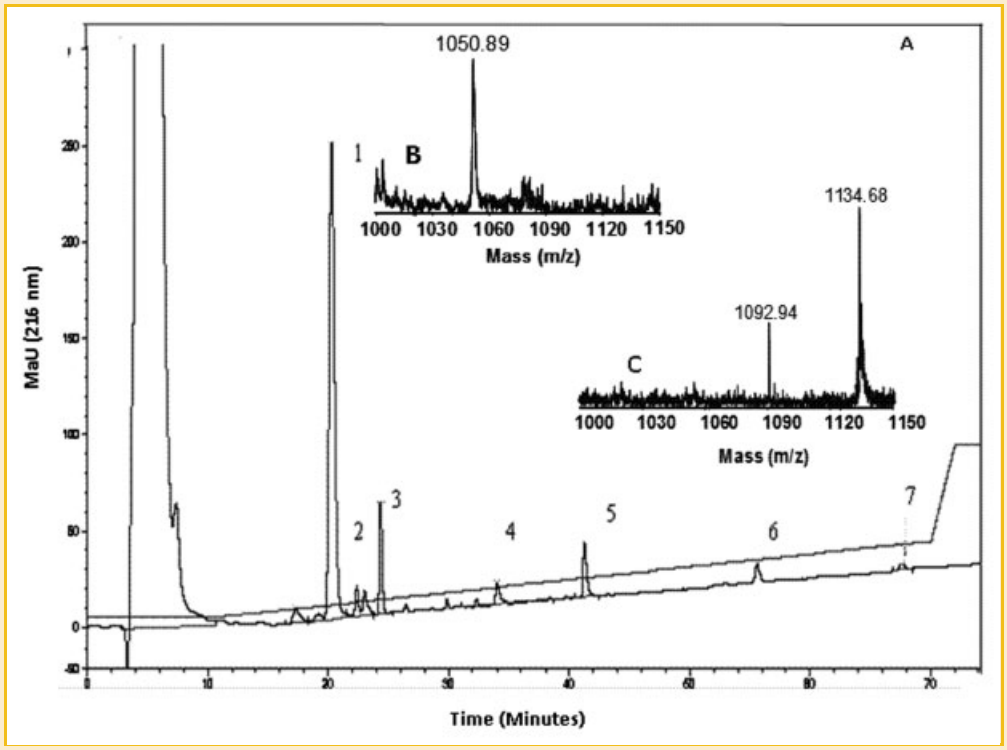

Fig. 1. HPLC profile (A) showing the elution profile of peptides <3 kDa, fractionated onto reversed phase HPLC with a ZORBAX-300SB-C18 column at a flow rate of 600 μl min^{-1}, by using a linear acetonitrile gradient (5–60%, v/v) as observed at diagonal line. MALDI-TOF mass spectra of peptide fraction 5 (*Cr*-ACP1) acquired in linear operating mode (B) and respective acetylated form (*Cr*-AcACP1) (C).

cultures. Apoptosis induction occurred in a time-dependent manner following peptide treatment. *Cr*-ACP1 increased apoptosis with long-term treatment as quantified by flow-cytometry (data not shown). This induction of programmed cell death was targeted on DNA ladder confirmed by fluorescent microscopy. Nucleosome deformation was observed under fluorescent microscopy after PI staining (Fig. 3). The observation of Hep2 cells at higher doses indicated loss of DNA after random DNA degradation. This result indicates that *Cr*-AcACP1 was more active than *Cr*-ACP1 to kill the cancerous cells.

Recent investigations have demonstrated that many apoptotic cascades utilize mitochondria as the nodal point where diverse apoptotic stimuli translate from initiation into execution undergo critical mitochondrial changes, including the collapse of the inner transmembrane potential, the generation of ROS, and the release of cytochrome *c* [Zorov et al., 2006]. Our results show that the exposure of Hep2 cells to *Cr*-ACP1 resulted in an improvement of apoptotic process verified from chromatin condensation and the assessment of sub-G0/G1 cells by FACS analysis. Earlier, Ellerby et al. [Ellerby et al., 1999] designed a synthetic peptide of 14-amino acids as KLAKLAKKLAKLAK, called $(KLAKLAK)_2$, where all-D enantiomer was used to avoid the degradation by proteases that preferentially disrupts mitochondrial membranes and induces mitochondria-dependent apoptosis. Thus, our result implies that *Cr*-ACP1 possibly acts as a chemopreventive agent, inducing inhibition of the growth of epidermoid carcinoma and colon carcinoma cells of apoptosis.

DNA BINDING ACTIVITY OF *Cr*-ACP1 AND *Cr*-AcACP1

Aiming to provide direct evidence for *Cr*-ACP1 and *Cr*-AcACP1's role in DNA binding, we performed EMSA. Figure 2b clearly shows that DNA binding activity increased as peptide concentration rose (0 mM, lane 1; 0.8 mM, lane 2; 1.0 mM, lane 3). This suggests that the DNA binding activity of *Cr*-AcACP1 was twice that of *Cr*-ACP1. Hence, DNA binding is the probable cause of apoptosis induction. Inactivation of oligonucleotides with functional peptides is an alternative and fascinating way to control cancer cells. Recently, NH–carbene complexes have started to contribute significant results in DNA binding and are being widely used as anticancer drugs; they are highly effective, but the patient is likely to suffer from severe side effects [Roy et al., 2009]. Complexation data provided here suggests that anticancer activity could be related to the process of peptide-DNA binding since *Cr*-ACP1 showed lower affinity to DNA in comparison to *Cr*-AcACP1. Anticancer activity was also improved at the same rate (Fig. 2A) with the presence of the acetyl group. In this context, natural peptides with DNA binding activity that induces apoptosis in the cancer cell seem to be more promising, as explained by in silico studies in the next topic.

ANTIMICROBIAL ACTIVITY

Another interesting issue observed here is peptide promiscuity, in which multiple functions are associated with a single molecule [Franco, 2011]. Since several plant peptides with similar physical–chemical properties to the peptide presented here have shown antimicrobial activity [Mandal et al., 2009; Otero-Gonzalez et al.,

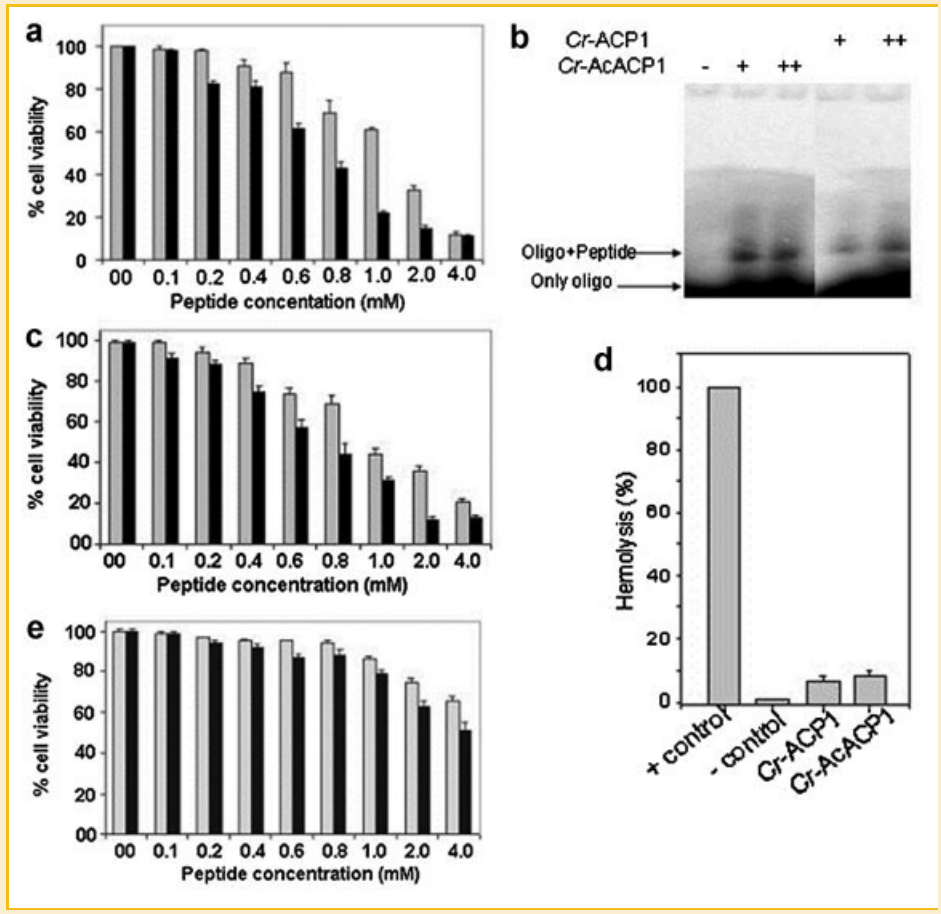

Fig. 2. Dose-dependent cytotoxic activity of *Cr*-ACP1 and *Cr*-AcACP1. Human epidermoid cancer cells (a); human colon carcinoma cells HCT15 (c), non-carcinoma mouse embryo fibroblast cells NIH 3T3 (e) were grown in vitro in 96-well plates and treated with different concentrations (0.0–4 mM) of peptide *Cr*-ACP1 (gray color) and *Cr*-AcACP1 (black color). The mean of the percentage cell viability (% of control) along with standard deviation of triplicate results are indicated. (b) Electro mobility shift assay for direct evidence of *Cr*-ACP1 and *Cr*-AcACP1's role in DNA binding. *Cr*-ACP1 and *Cr*-AcACP1 were incubated with oligo, 5′-P32-labeled (5′-CCG GGG CAG GGC TTA GGT CT-3′) at a concentration of 0 mM (lane 1), 0.8 mM (lane 2), and 1.0 mM (lane 3). Results indicate that binding activity rose with increasing peptide concentrations and *Cr*-AcACP1 was more active than only *Cr*-ACP1. (d) Hemolytic assay of *Cr*-ACP1 and *Cr*-AcACP1. The concentration of peptides were used at 1 mM and incubated for 30 min at 37°C. Data are the mean of triplicates ± SD.

2010; Moreira et al., 2011; Ribeiro et al., 2011], we also evaluated the antimicrobial activity of *Cr*-ACP1. The antimicrobial activity of both peptides was evaluated in vitro against four different human pathogenic bacteria (Table I) showing that the acetylated form of *Cr*-AcACP1 is less active than *Cr*-ACP1, in contrast to anticancer activity, which was improved by the presence of acetyl groups. The non-acetylated form showed higher potency toward *B. subtilis*, *P. aeruginosa*, and *E. coli* (MIC 30 μM) and lower against *S. epidermidis* (MIC 60 μM). These are a low MICs values when compared to other antibacterial proteins. For example, potamin-1 (PT-1), a peptide from *Solanum tuberosum* which caused deleterious effects against *Clavibacter michiganensis* development, showed an MIC of 50 μM [Kim et al., 2005]. Moreover is important to cite that all strains affected by Cr-ACP1 are opportunistic human pathogens. *S. epidemidis* is one of the most prevalent cutaneous resident bacteria, being extremely resistant to conventional antibiotics. Several studies have been identified *S. epidermidis* as a common opportunistic pathogen of human skin that easily colonize on the indwelling catheters surface, prosthetic joints, cerebrospinal fluid shunts [Schoenbaum et al., 1975]. Moreover *P. aeruginosa*, is able to cause lung infections, cystic fibrosis, nosocomial infections, and a wide range of severe and sometimes fatal diseases in immunocompromised individuals [Cappello and Guglielmino, 2006]. Finally, *B. subtilis* and *E. coli* may cause serious food poisoning suggesting that peptide here reported could be usefully for the treatment of multiple human infections.

In addition to a comparison between antimicrobial potencies, it is also important to compare the effects of acetyl groups over the bactericidal activities. It seems that acetylation was harmful to bactericidal activity due to the blocking of amino acid residue Lys^3 as here observed in Table I. This modification entails an imbalance in the total charge preventing an electrostatic approximation to the target. This result has also been observed in recent research that evaluated the role of acetylation and charge exposition in antimicrobial peptides based on human β-defensin-3. Despite of their higher potency, when compared to *Cr*-AMP1, the acetylated peptide, named Pep-1, showed an EC_{50} value of 32 μM and for the non-acetylated Pep-1 this was 2 μM [Papanastasiou et al., 2009]

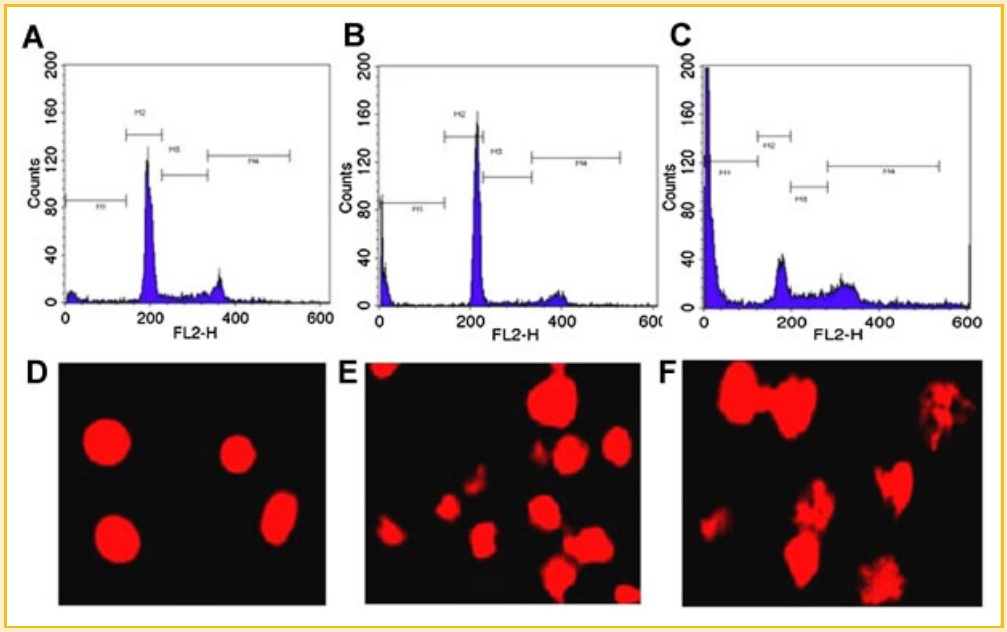

Fig. 3. Representative histogram plot of Hep2 cancer cells treated with *Cr*-ACP1 and *Cr*-AcACP1 (0.8 mM) for 24 h. Control (0.1% DMSO) cultures (A), *Cr*-ACP1 (B), and *Cr*-AcACP1 (C) indicating more cell cycle arrest at the G0–G1 phase in epidermoid cancer cells with *Cr*-AcACP1. Fluorescent microscopic analysis of DNA fragmentation and apoptosis by of Hep2 cells treated with control (0.1% DMSO), (D); 0.8 mM of *Cr*-ACP1 (E) and *Cr*-AcACP1(F).

corroborating data here presented that acetylation group could reduce the effectiveness of some antimicrobial peptides.

This surprising and unexpected secondary function could be explained by peptide promiscuity, observed in several other plant antimicrobial peptides, such as defensins, cyclotides, and 2S albumins [Franco, 2011], suggesting that these peptides could bind to different targets. These data suggest that this peptide could be used in the development of a therapeutic treatment against microorganisms and, due to the low concentration needed, may produce fewer toxic side effects.

MOLECULAR MODELING AND DOCKING OF PEPTIDES AND ssDNA

The 3D model of anticancer peptides showed 44% and 22% of identity with structures deposited in Protein Data Bank (http://www.pdb.org/pdb/home/home.do), with pdb code 1d9j and 1b1v, respectively, which were chemically synthesized and the 3D structures resolved by NMR. The peptide pdb: 1d9j is a hybrid of antimicrobial sequences of cecropin-A (1-8 residue)—magainin-2 (1-12 residue) which naturally occurs in *Hyalophora cecropia* and *Xenopus laevis*, and pdb: 1b1v is an insect cytokine peptide which may be found naturally in the hemolymph tissue of *Pseudoplusia includens*. The validation of the 3D model of peptide anticancer by Ramachandran plot showed that in the model presented 100% of the amino acid residues are in physically acceptable regions for secondary structure formation in relation to torsion angles phi and psi. The z-score value in PROSA II program can be used to check whether the input structure is within the range of scores typically found for native proteins of similar size. The z-score value was 0.8, compared with NMR structures in anticancer peptides of similar length (z-score 1 to −1.5) [Hwang et al., 1998; Kristiansen et al., 2005; Wang et al., 2005]. The values of RMSD for anticancer peptide were 1.63 and 1.02 Å.

TABLE I. Antimicrobial Activities of *Cr*-ACP1 and *Cr*-AcACP1 Peptides

	MIC values (μM)	
Bacteria	*Cr*-ACP1	*Cr*-AcACP1
S. epidermidis	60	230
B. subtilis	30	58
P. aeruginosa	30	58
E. coli	30	116

All assays were performed in triplicate do not differing more than 5%.

The 3D non-acetylated anticancer peptide model presented cationic (Lys^3) and aromatic (Trp^2) residues forming a single amphipathic α-helice that showed 55% of hydrophobic residues. This structural fold is commonly found in peptides with multiple activities such as antimicrobial, antifungal, and antitumoral [Rodrigues et al., 2009]. Helene and Maurizot [Helene and Maurizot, 1981] have observed that short oligopeptides containing basic and aromatic residues provided simple systems where it was possible to differentiate between single-stranded and double-stranded structures by inserting their aromatic residue between successive bases. On the other hand, the acetylated peptide presented an identical structural scaffold. For model construction, in accordance with MS data (Fig. 1), two acetyl groups were added, the first being linked to Ala^1 and the second bound to Lys^3.

The interactions observed between DNA and acetylated and non-acetylated peptides were analyzed in silico. The interactions between non-acetylated peptide-ssDNAs suggest that the peptide

interacts with the sequence 5′-CCGGC-3′ of ssDNA through residues Ala[1], Lys[3], and Asp[6] of *Cr*-AcACP1 (Fig. 4A). In summary, the DNA O3′ atom receptors of G[9] interact with the nitrogen atom of the main chain of amino acid residue Ala[1] with 2.72 Å. The atoms 1HZ and 2HZ of NZ Lys[3] lateral chain residue interact by N1 and O6 of nitrogen base G[9], forming hydrogen bonds with 1.89 and 3.19 Å. Hydrogen interactions were observed in N1 and N2 of nitrobase G[6] with atoms at Asp[6] lateral chain residue OD1 and OD2, which present 2.93 and 2.56 Å, respectively, with stabilization of peptide forward ssDNA, showing an interaction surface area of 50 Å^2. This indicates once more that the hydrogen bonding net observed here plays an essential role in the binding and stabilization of peptides with a ssDNA. The Trp[2] residue was positioned between two hydrophilic branches and inserted into two nucleotide bases that assist in a "hydrophilic hug." Coleman and Oakley [1980] observed that this might be an important factor in the recognition of single-stranded nucleic acids by single-strand binding proteins. The insertion of an aromatic amino acid side chain into an apurinic site might form the basis for the selective recognition of such sites in apurinic DNA [Behmoaras et al., 1981b]. As observed with the peptide isolated here, the presence of hydrophobic residues surrounding cationic residues is observed in 80% of peptides with anticancer activity deposited on APD2 [Behmoaras et al., 1981a].

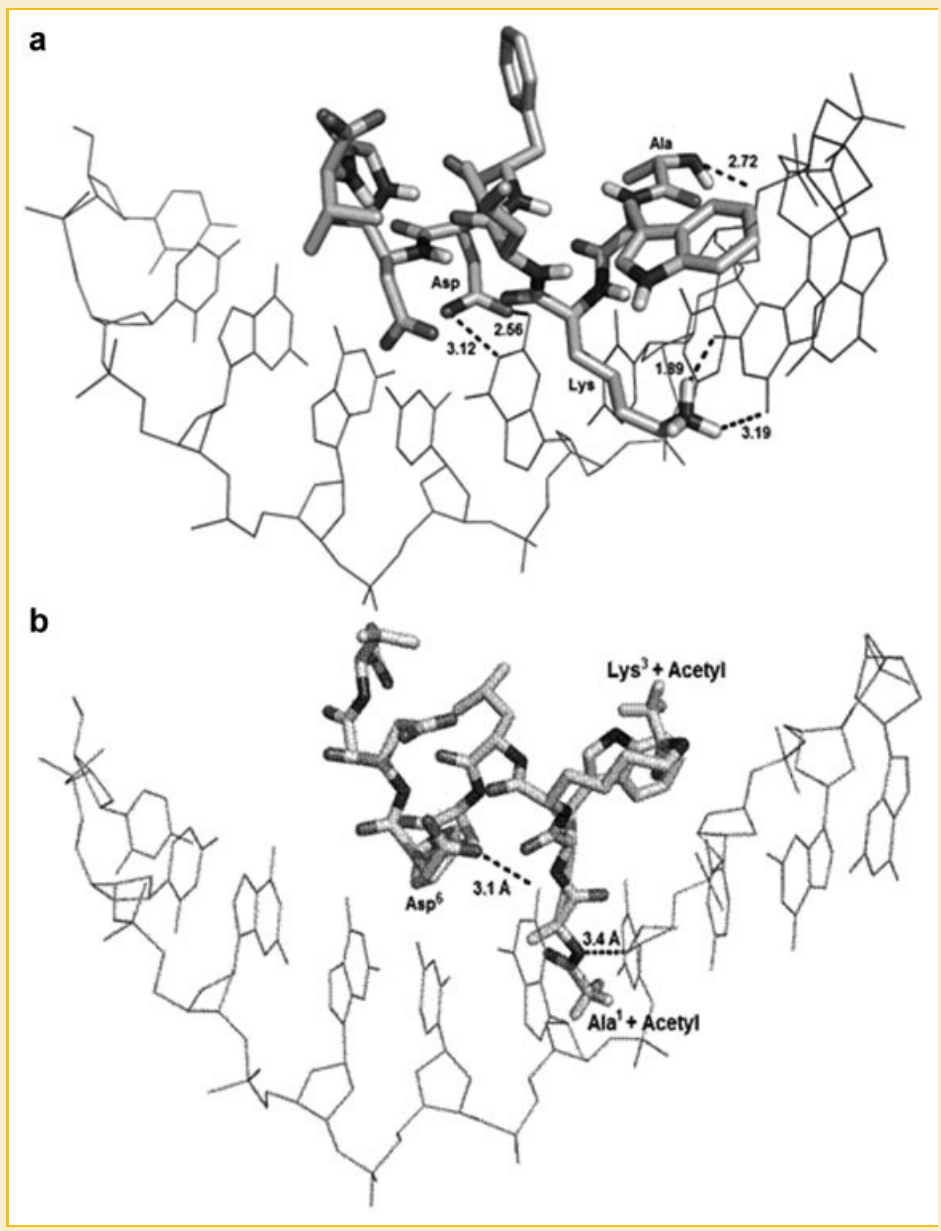

Fig. 4. Theoretical docking studies showing the binary complex formed between *Cr*-ACP1 (a) and *Cr*-AcACP1 (b) anticancer peptides with a single stranded DNA 5′-CCGGC-3′. Peptide and DNA are represented in ball stick format. Lateral chains involved in complex formation are labeled. Dotted lines indicate hydrogen bonds and respective distances in angstroms. Pymol program was used for visualization.

The interaction observed for acetylated peptide with ssDNA showed weak affinity to bacteria, when compared to *Cr*-ACP1, as observed in in vitro assays. An explanation for this lower interaction between acetylated peptide and bacteria suggests that acetylation at Lys^3 may block residue action due to a modification in charge surface. On the other hand, the affinity observed in the electro mobility shift assay between *Cr*-AcACP1 and ssDNA was twice as high as that for *Cr*-ACP1, indicating that DNA interaction and antimicrobial activity are not directly related. *Cr*-AcACP1 showed the formation of a hydrogen bond between Ala^1 (O) amino acid residue in N-termini and hydroxyl (O6) of DG^4 nucleotide with distance of 3.22 Å. The oxygen of acetyl group linked to Lys^3 formed a hydrogen bond with N2 of DG^4 with distance of 1.64 Å. A new interaction was also observed only in the acetylated form between oxygen (O) of Trp^2 and N2 of DG^6 with distance of 3.39 Å. In addition, two other hydrogen bonds were observed. The first was proposed between the oxygen donor (OD2) in Asp^6 residue and the receptor (O2) in DC^7, and the second between the oxygen donor (OD1) in Asp^7 residue and the receptor OP1 DC^8 with distances of 3.28 and 3.46 Å, respectively (Fig. 4B). The interaction surface area observed between *Cr*-AcACP1 and ssDNA was 60 $Å^2$ higher than the interaction between *Cr*-ACP1 and ssDNA suggesting a major affinity, as observed in gel experiments (Fig. 2B).

Although the acetylated peptide studied here has shown higher ability to bind to DNA, some contrary results have previously been observed. For example, the N-terminal acetylation of peptides derived from histone H4 showed that the peptide lost the capability to link DNA after acetylation due to the electrostatic change that leads the chromatin to an extended form, reducing the interaction [Cary et al., 1982].

CONCLUSIONS

In conclusion, the present work aimed to identify a novel promiscuous peptide with anticancerous and bactericidal activity isolated from plant seeds. It was clearly observed that the peptide exhibited significant apoptotic activity in addition to DNA binding property, indicating that further modifications of these compounds may be promising candidates for clinical drug agents. These adaptations could improve the activity and also the specificity, transforming peptide here reported in a possible biopharmacy. However, at this moment, it is impossible to forecast the utilization of this peptide since modifications such as acetylation reduced the peptide's effectiveness against bacteria. This data suggest the importance of N-termini for functional development. Otherwise, the acetylated peptide showed higher affinity to DNA and also improved anticancer activity, indicating that two indirectly related different targets are observed here. Data reported in this work give the probable mechanisms of interaction obtained by in silico studies. These analyses demonstrated the ability to satisfactorily interact with ssDNA, indicating that the role of the amino acid residues Ala^1, Trp^2, Lys^3, Asp^6, and Asp^7 is important for the stabilization complex, in addition to the presence of an acetyl group. Therefore the small peptide can block DNA replication and inhibit cancer development, especially in its acetylated form. This information adds to the available knowledge about anticancer plant peptides, and it should be validated by NMR technology in the near future to construct novel therapeutic treatments to combat cancer's devastating effects.

REFERENCES

Behmoaras T, Toulme JJ, Helene C. 1981a. Specific recognition of apurinic sites in DNA by a tryptophan-containing peptide. Proc Natl Acad Sci USA 78:926–930.

Behmoaras T, Toulme JJ, Helene C. 1981b. A tryptophan-containing peptide recognizes and cleaves DNA at apurinic sites. Nature 292:858–859.

Cappello S, Guglielmino SPP. 2006. Effects of growth temperature on polystyrene adhesion of *Pseudomonas aeruginosa* ATCC 27853. Braz J Microbiol 37:205–207.

Cary PD, Crane-Robinson C, Bradbury EM, Dixon GH. 1982. Effect of acetylation on the binding of N-terminal peptides of histone H4 to DNA. Eur J Biochem 127:137–143.

Coleman JE, Oakley JL. 1980. Physical chemical studies of the structure and function of DNA binding (helix-destabilizing) proteins. CRC Crit Rev Biochem 7:247–289.

Ellerby HM, Arap W, Ellerby LM, Kain R, Andrusiak R, Rio GD, Krajewski S, Lombardo CR, Rao R, Ruoslahti E, Bredesen DE, Pasqualini R. 1999. Anticancer activity of targeted pro-apoptotic peptides. Nat Med 5:1032–1038.

Espinosa E, Morales S, Borrega P, Casas A, Madronal C, Machengs I, Illarramendi JA, Lizon J, Moreno JA, Belon J, Janariz J, de la Puente M, Checa T, Mel JR, Gonzalez Baron M. 2004. Docetaxel and high-dose epirubicin as neoadjuvant chemotherapy in locally advanced breast cancer. Cancer Chemother Pharmacol 54:546–552.

Feliu L, Oliveras G, Cirac AD, Besalu E, Roses C, Colomer R, Bardaji E, Planas M, Puig T. 2010. Antimicrobial cyclic decapeptides with anticancer activity. Peptides 31:2017–2026.

Franco OL. 2011. Peptide promiscuity: An evolutionary concept for plant defense. FEBS Lett 585:995–1000.

Gong B, Ramos A, Vazquez-Fernandez E, Silva CJ, Alonso J, Liu Z, Requena JR. 2011. Probing structural differences between PrPC and PrPSc by surface nitration and acetylation: Evidence of conformational change in the C-terminus. Biochemistry 50(22):4963–4972.

Helene C, Maurizot JC. 1981. Interactions of oligopeptides with nucleic acids. CRC Crit Rev Biochem 10:213–258.

Hwang PM, Zhou N, Shan X, Arrowsmith CH, Vogel HJ. 1998. Three-dimensional solution structure of lactoferricin B, an antimicrobial peptide derived from bovine lactoferrin. Biochemistry 37:4288–4298.

Ireland DC, Clark RJ, Daly NL, Craik DJ. 2010. Isolation, sequencing, and structure-activity relationships of cyclotides. J Nat Prod 73:1610–1622.

Johnson CA, Turner BM. 1999. Histone deacetylases: Complex transducers of nuclear signals. Semin Cell Dev Biol 10(2):179–188.

Kaplan W, Littlejohn TG. 2001. Swiss-PDB viewer (deep view). Brief Bioinform 2:195–197.

Kerkis I, Silva Fde S, Pereira A, Kerkis A, Radis-Baptista G. 2010. Biological versatility of crotamine—A cationic peptide from the venom of a South American rattlesnake. Expert Opin Investig Drugs 19:1515–1525.

Kim JY, Park SC, Kim MH, Lim HT, Park Y, Hahm KS. 2005. Antimicrobial activity studies on a trypsin-chymotrypsin protease inhibitor obtained from potato. Biochem Biophys Res Commun 330:921–927.

Kristiansen PE, Fimland G, Mantzilas D, Nissen-Meyer J. 2005. Structure and mode of action of the membrane-permeabilizing antimicrobial peptide pheromone plantaricin A. J Biol Chem 280:22945–22950.

Kues WA, Anger M, Carnwath JW, Paul D, Motlik J, Niemann H. 2000. Cell cycle synchronization of porcine fetal fibroblasts: Effects of serum deprivation and reversible cell cycle inhibitors. Biol Reprod 62(2):412–419.

Laskowski RA, Rullmannn JA, MacArthur MW, Kaptein R, Thornton JM. 1996. AQUA and PROCHECK-NMR: Programs for checking the quality of protein structures solved by NMR. J Biomol NMR 8:477–486.

Mader JS, Ewen C, Hancock RE, Bleackley RC. 2011. The human cathelicidin, LL-37, induces granzyme-mediated apoptosis in regulatory T cells. J Immunother 34:229–235.

Mandal SM, Dey S, Mandal M, Sarkar S, Maria-Neto S, Franco OL. 2009. Identification and structural insights of three novel antimicrobial peptides isolated from green coconut water. Peptides 30:633–637.

Mandal SM, Dey S, Mandal M, Maria-Neto S, Franco OL. 2010. Comparative analyses of different surfactants on matrix-assisted laser desorption/ionization mass spectrometry peptide analysis. Eur J Mass Spectrom (Chichester, Eng) 16:567–575.

Mandal SM, Migliolo L, Franco OL, Ghosh AK. 2011. Identification of an antifungal peptide from *Trapa natans* fruits with inhibitory effects on *Candida tropicalis* biofilm formation. Peptides 32(8):1741–1747.

Moreira JS, Almeida RG, Tavares LS, Santos MO, Viccini LF, Vasconcelos IM, Oliveira JT, Raposo NR, Dias SC, Franco OL. 2011. Identification of botryticidal proteins with similarity to NBS-LRR proteins in rosemary pepper (*Lippia sidoides* Cham.) flowers. Protein J 30:32–38.

Morris AL, MacArthur MW, Hutchinson EG, Thornton JM. 1992. Stereochemical quality of protein structure coordinates. Proteins 12:345–364.

Oh D, Shin SY, Kang JH, Hahm KS, Kim KL, Kim Y. 1999. NMR structural characterization of cecropin A(1-8)—Magainin 2(1-12) and cecropin A (1-8)—Melittin (1-12) hybrid peptides. J Pept Res 53:578–589.

Otero-Gonzalez AJ, Magalhaes BS, Garcia-Villarino M, Lopez-Abarrategui C, Sousa DA, Dias SC, Franco OL. 2010. Antimicrobial peptides from marine invertebrates as a new frontier for microbial infection control. FASEB J 24: 1320–1334.

Paganuzzi AS, Zucco F, Cardelli M, de Angelis I, Mattei R, Pino A, Rocca E, Zampaglioni F. 1985. Cytotoxic effects of wheat gliadin-derived peptides. Toxicology 37:225–232.

Papanastasiou EA, Hua Q, Sandouk A, Son UH, Christenson AJ, Van Hoek ML, Bishop BM. 2009. Role of acetylation and charge in antimicrobial peptides based on human beta-defensin-3. APMIS 117:492–499.

Perera Y, Farina HG, Gil J, Rodriguez A, Benavent F, Castellanos L, Gomez RE, Acevedo BE, Alonso DF, Perea SE. 2009. Anticancer peptide CIGB-300 binds to nucleophosmin/B23, impairs its CK2-mediated phosphorylation, and leads to apoptosis through its nucleolar disassembly activity. Mol Cancer Ther 8:1189–1196.

Preza AM, Jaramillo ME, Puebla AM, Mateos JC, Hernandez R, Lugo E. 2010. Antitumor activity against murine lymphoma L5178Y model of proteins from cacao (*Theobroma cacao* L.) seeds in relation with in vitro antioxidant activity. BMC Complement Altern Med 10:61. Available at: http://www.ncbi.nlm.nih.gov/pubmed/20961452

Purcell AW, McCluskey J, Rossjohn J. 2007. More than one reason to rethink the use of peptides in vaccine design. Nat Rev Drug Discov 6: 404–414.

Rawat DS, Joshi MC, Joshi P, Atheaya H. 2006. Marine peptides and related compounds in clinical trial. Anticancer Agents Med Chem 6:33–40.

Rees WA, Keller RW, Vesenka JP, Yang G, Bustamante C. 1993. Evidence of DNA bending in transcription complexes imaged by scanning force microscopy. Science 260:1646–1649.

Ribeiro SM, Almeida RG, Pereira CA, Moreira JS, Pinto MF, Oliveira AC, Vasconcelos IM, Oliveira JT, Santos MO, Dias SC, Franco OL. 2011. Identification of a *Passiflora alata* Curtis dimeric peptide showing identity with 2S albumins. Peptides 32:868–874.

Ritchie DW. 2008. Recent progress and future directions in protein-protein docking. Curr Protein Pept Sci 9:1–15.

Rodrigues EG, Dobroff AS, Taborda CP, Travassos LR. 2009. Antifungal and antitumor models of bioactive protective peptides. An Acad Bras Cienc 81: 503–520.

Roy S, Maheswari PU, Lutz M, Spek AL, den Dulk H, Barends S, van Wezel GP, Hartl F, Reedijk J. 2009. DNA cleavage and antitumour activity of platinum(II) and copper(II) compounds derived from 4-methyl-2-N-(2-pyridylmethyl) aminophenol: Spectroscopic, electrochemical and biological investigation. Dalton Trans 28:10846–10860.

Roy A, Kucukural A, Zhang Y. 2010. I-TASSER: A unified platform for automated protein structure and function prediction. Nat Protoc 5:725–738.

Rozek T, Wegener KL, Bowie JH, Olver IN, Carver JA, Wallace JC, Tyler MJ. 2000. The antibiotic and anticancer active aurein peptides from the Australian Bell Frogs *Litoria aurea* and *Litoria raniformis* the solution structure of aurein 1.2. Eur J Biochem 267:5330–5341.

Sartorius J, Schneider HJ. 1995. NMR-titrations with complexes between ds-DNA and indole derivatives including tryptophane containing peptides. FEBS Lett 374:387–392.

Schoenbaum SC, Gardner P, Shillito J. 1975. Infection of cerebrospinal fluid shunts: Epidemiology, clinical manifestations and therapy. J Infect Dis 131: 543–552.

Sumathi K, Ananthalakshmi P, Roshan MN, Sekar K. 2006. 3dSS: 3D structural superposition. Nucleic Acids Res 34:W128–W132.

Tan J, Wang B, Zhu L. 2009. DNA binding, cytotoxicity, apoptotic inducing activity, and molecular modeling study of quercetin zinc(II) complex. Bioorg Med Chem 17:614–620.

Torchilin VP, Lukyanov AN. 2003. Peptide and protein drug delivery to and into tumors: Challenges and solutions. Drug Discov Today 8:259–266.

Volkman BF, Anderson ME, Clark KD, Hayakawa Y, Strand MR, Markley JL. 1999. Structure of the insect cytokine peptide plasmatocyte-spreading peptide 1 from *Pseudoplusia includens*. J Biol Chem 274:4493–4496.

Wang G, Li Y, Li X. 2005. Correlation of three-dimensional structures with the antibacterial activity of a group of peptides designed based on a nontoxic bacterial membrane anchor. J Biol Chem 280:5803–5811.

Wikler MA, Low DE, Cockerill FR, Sheehan DJ, Craig WA, Tenover FC, Dudley MN. 2005. Methods for dilution antimicrobial susceptibility tests for bacteria that grow aerobically: Approved standard-sixth edition, Vol. 29. Pennsylvania: Clinical and Laboratory Standards Institute. ISBN No. 1-56238-689-1.

Wu JM, Jan PS, Yu HC, Haung HY, Fang HJ, Chang YI, Cheng JW, Chen HM. 2009. Structure and function of a custom anticancer peptide, CB1a. Peptides 30:839–848.

Yang D, Wang AH. 1996. Structural studies of interactions between anticancer platinum drugs and DNA. Prog Biophys Mol Biol 66:81–111.

Yokoyama S, Kato K, Koba A, Minami Y, Watanabe K, Yagi F. 2008. Purification, characterization, and sequencing of antimicrobial peptides, Cy-AMP1, Cy-AMP2, and Cy-AMP3, from the Cycad (*Cycas revoluta*) seeds. Peptides 29:2110–2117.

Yokoyama S, Iida Y, Kawasaki Y, Minami Y, Watanabe K, Yagi F. 2009. The chitin-binding capability of Cy-AMP1 from cycad is essential to antifungal activity. J Pept Sci 15:492–497.

Zorov DB, Juhaszova M, Sollott SJ. 2006. Mitochondrial ROS-induced ROS release: An update and review. Biochim Biophys Acta 1757:509–517.